Iterative Frequency-Domain Channel Estimation and Equalization for Single-Carrier Transmissions without Cyclic-Prefix

Hong Liu and Philip Schniter

***Abstract*—Compared to conventional time-domain equalization, frequency-domain equalization (FDE) presents a computationally efficient alternative for the reception of single carrier (SC) transmissions. In this paper, we consider iterative FDE (IFDE) with explicit frequency-domain channel estimation (FDCE) for non-cyclic-prefixed SC systems. First, an improved IFDE algorithm is presented based on soft iterative interference-cancellation. Second, a new adaptive FDCE (AFDCE) algorithm based on per-tone Kalman filtering is proposed to track and predict the frequency-domain channel coefficients. The AFDCE algorithm employs across-tone noise reduction, exploits temporal correlation between successive blocks, and adaptively updates the auto-regressive model coefficients, bypassing the need for prior knowledge of channel statistics. Finally, block-overlapping is used to facilitate the joint operation of IFDE and AFDCE. Simulation results show that, compared to related IFDE and adaptive channel estimation schemes, the proposed schemes offer lower mean-square error (MSE) in channel prediction, lower bit error rate (BER) after decoding, and robustness to non-stationary channels.**

***Index Terms*—Iterative frequency-domain equalization, frequency-domain channel estimation, Kalman filter, MMSE, single carrier, time-varying frequency-selective channels.**

I. Introduction

BROADBAND wireless access systems offering high data-rates are likely to face severe multipath fading, including channel delay spreads spanning tens or hundreds of symbol intervals. While orthogonal frequency division multiplexing (OFDM) is a popular means of combating these multipath effects, its drawbacks include high peak-to-average power ratio (PAPR) and high sensitivity to carrier-frequency offset (CFO). Single carrier (SC) transmission with frequency-domain equalization (FDE) presents an alternative to OFDM that retains robustness to delay spread without the disadvantages of high PAPR and CFO-sensitivity [1]. SC transmission without cyclic prefix (CP) [2] offers, in addition, spectral efficiency advantages relative to CP-based OFDM systems. When FDE is accomplished via turbo equalization (TE) [3], [4], an iterative reception scheme whereby the equalizer and decoder iteratively exchange soft information to jointly exploit channel structure and code structure, significant performance gains result with only modest increase in demodulator complexity [5], [6]. Hence, the focus of this paper is SC transmission with turbo FDE.

Manuscript received April 6, 2007; revised December 18, 2007 and May 11, 2008; accepted July 8, 2008. The associate editor coordinating the review of this paper and approving it for publication was H. Nguyen. This work was supported by the National Science Foundation under Grant No. 0237037. This paper was presented in part at the Conference on Information Sciences and Systems, Baltimore, MD, March 2007.

The authors are with the Department of Electrical and Computer Engineering, Ohio State University, Columbus, OH (e-mail: schniter@ece.osu.edu).

Digital Object Identifier 10.1109/T-WC.2008.070371

When targeting practical implementation, accurate and efficient channel estimation (CE) is critical. For OFDM systems, various frequency-domain channel estimation (FDCE) schemes have been proposed to track and predict either slow-fading or fast-fading wireless channels, with or without pilot symbols, and with or without knowledge of channel statistics [7]–[9]. For SC systems, time-domain channel estimation is the typical approach [10]–[12], though a few pilot-aided FDCE schemes have been proposed [13]–[15].

In this paper, we propose a new joint channel-estimation/equalization scheme for the reception of SC transmissions over wireless channels with relatively fast fading and long delay spread. First, an improved iterative FDE (IFDE) algorithm based on frequency-domain TE is presented. Second, a new adaptive FDCE (AFDCE) algorithm based on per-tone Kalman filtering and across-tone noise reduction is proposed. The AFDCE also exploits the temporal correlation between successive blocks and adaptively updates the channel's auto-regressive (AR) model [16] coefficients when they are unknown or varying. Finally, to facilitate the joint operation of IFDE and AFDCE, a block-overlapping scheme is used. Our approach differs from related work for single-carrier systems in the following three ways. 1) Existing IFDE algorithms [2], [5], [6] are derived in the time domain and approximated in the frequency domain, while our IFDE algorithm is derived in the frequency domain directly. 2) Existing CE algorithms work [10]–[12] in the time domain, while ours works in the frequency domain, thereby reducing complexity for long delay spread channels. 3) Existing FDCEs [13]–[15] are pilot-aided. Since the use of pilots decreases spectral efficiency, we consider CE that is exclusively decision-directed.

II. System Model

Consider[1] coded single-carrier transmission where a bit stream $\{b_m\}$ is coded and mapped to symbols $\{s_n\}$ in a finite alphabet $\mathcal{S}$ and transmitted over a noisy linear time-varying multipath wireless channel. For simplicity, we assume $\{s_n\}$ to be uncorrelated. The complex-baseband channel can be described by the time-varying length-N_h impulse response $\{h_{n,l}\}_{l=0}^{N_h-1}$, where $h_{n,l}$ denotes the time-n response to an impulse applied at time $n-l$. The complex-valued observations

[1]*Notation:* Upper (lower) bold face letters are used for matrices (column vectors). $\boldsymbol{A}^*$, $\boldsymbol{A}^T$, $\boldsymbol{A}^H$ and $\boldsymbol{A}^{-1}$ denote the conjugate, transpose, Hermitian transpose, and inverse of $\boldsymbol{A}$, respectively. $\boldsymbol{I}$ denotes the identity matrix, $\boldsymbol{i}_n$ the nth column of $\boldsymbol{I}$, and $\boldsymbol{F}$ the unitary $N \times N$ discrete Fourier transform (DFT) matrix. $\mathcal{C}(\boldsymbol{a})$ denotes the convolution matrix constructed with first column $\boldsymbol{a}$, $\mathcal{D}(\boldsymbol{a})$ the diagonal matrix constructed from vector $\boldsymbol{a}$, and $\mathrm{diag}(\boldsymbol{A})$ the vector formed from the diagonal elements of square matrix $\boldsymbol{A}$. δ_p denotes the Kronecker delta, and $\langle n \rangle_N$ denotes n-modulo-N. Finally, $\mathcal{CN}(\boldsymbol{\mu}, \boldsymbol{\Sigma})$ denotes the multi-dimensional circular Gaussian distribution with mean $\boldsymbol{\mu}$ and covariance $\boldsymbol{\Sigma}$.

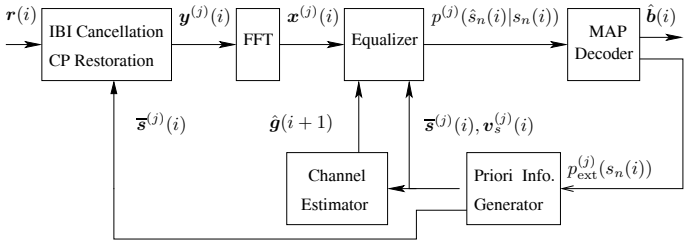

Fig. 1. Receiver structure.

$\{r_n\}$ are then given by $r_n = \sum_{l=0}^{N_h-1} h_{n,l}s_{n-l} + \nu_n$,where $\{\nu_n\}$ is zero-mean circular white Gaussian noise with variance σ_w^2. Note that this describes SC transmission without cyclic prefix.

To implement IFDE and AFDCE jointly, we use overlapped block-processing with block length N and block shift interval $N_d < N$ (discussed in Section VI-A). Furthermore, we consider channel time-variation slow enough to model the channel as time-invariant within the N-block. In terms of the block-based quantities $r_n(i) = r_{iN_d+n}$, $s_n(i) = s_{iN_d+n}$, $\nu_n(i) = \nu_{iN_d+n}$, and $h_l(i) = h_{iN_d+\frac{N}{2},l}$ (sampling the channel in the middle[2] of the N-block), the signal received during the ith block can be expressed as $r_n(i) =$

$$\begin{cases} \nu_n(i) + \displaystyle\sum_{l=0}^{n} h_l(i)s_{n-l}(i) + \sum_{l=n+1}^{N_h-1} h_l(i)s_{\langle n-l\rangle_N}(i-1), \\ \qquad\qquad 0 \le n < N_h - 1, \\ \nu_n(i) + \displaystyle\sum_{l=0}^{N_h-1} h_l(i)s_{n-l}(i), \qquad N_h - 1 \le n < N. \end{cases} \tag{1}$$

Note that $\{r_n(i)\}_{n=0}^{N_h-2}$ contains inter-block interference (IBI), i.e., symbol contributions from the previous block. In the sequel, we will make extensive use of the N-dimensional vectors $\boldsymbol{r}(i) := [r_0(i), \ldots, r_{N-1}(i)]^T$, $\boldsymbol{s}(i) := [s_0(i), \ldots, s_{N-1}(i)]^T$, $\boldsymbol{\nu}(i) := [\nu_0(i), \ldots, \nu_{N-1}(i)]^T$, and $\boldsymbol{h}(i) := [h_0(i), \ldots, h_{N_h-1}(i), 0, \ldots, 0]^T$.

III. Receiver Structure

The proposed receiver processing is illustrated in Fig. 1 and the corresponding processing steps are described below (for the ith block). Since the entire procedure can be repeated several times per block, the superscript j is used to denote the iteration index.

S1) Perform IBI-cancellation and CP-restoration on $\boldsymbol{r}(i)$ using the methods of [17], [18].

S2) With the aid of FFTs, perform frequency-domain MMSE equalization assuming symbol means and variances obtained through the previous round of decoding. From the time-domain symbol estimates $\hat{\boldsymbol{s}}(i)$, extract the conditional probabilities $\left\{p^{(j)}\left(\hat{s}_n(i)|s_n(i)=s\right), \forall s \in \mathcal{S}\right\}_{n=0}^{N-1}$ for use in decoding.

S3) Perform maximum *a posteriori* (MAP) decoding, and update the extrinsic *a priori* distribution $p_{\text{ext}}^{(j)}(s_n(i))$.

[2]For a slowly-varying channel, we reason that the channel sample in the middle of a block is most representative of the channel during that block.

S4) Using $p_{\text{ext}}^{(j)}(s_n(i))$, generate symbol means $\overline{\boldsymbol{s}}^{(j)}(i)$ and variances $\boldsymbol{v}_s^{(j)}(i)$ to be used as priors in the next round of equalization.

S5) Generate hard decisions from $\overline{\boldsymbol{s}}^{(j)}(i)$ and use them to smooth the current channel estimates and predict the channel for the next block.

For Step S3, we assume that the LOGMAP algorithm [19] is used for MAP decoding and that the the *a priori* distribution is generated in the standard way (see, e.g., [4]). In the following two sections, we describe the IFDE algorithm (Steps S1, S2, and S4) and the AFDCE algorithm (Step S5) in detail.

IV. Iterative Frequency-Domain Equalization

Throughout this section, we will assume perfect knowledge of the channel coefficients $\{h_l(i)\}_{l=0}^{N_h-1}$. In Section V, we detail how channel estimates and their errors are computed and incorporated into IFDE.

Our IFDE begins with IBI-cancellation and CP-reconstruction. As with the RISIC algorithm [17], we perform IBI-cancellation with $\{\hat{s}_n(i-1)\}$—the final estimates of previous-block symbols, and CP-reconstruction with $\{\bar{s}_n^{(j-1)}(i)\}$—the most recent estimates of current-block symbols, according to $y_n^{(j)}(i) =$

$$\begin{cases} r_n(i) - \displaystyle\sum_{l=n+1}^{N_h-1} h_l(i)\hat{s}_{\langle n-l\rangle_N}(i-1) + \sum_{l=n+1}^{N_h-1} h_l(i)\bar{s}_{\langle n-l\rangle_N}^{(j-1)}(i) \\ \qquad\qquad 0 \le n < N_h - 1 \\ r_n(i) \qquad\qquad N_h - 1 \le n < N \end{cases} \tag{2}$$

When $j = 1$, $\overline{\boldsymbol{s}}^{(j-1)}(i)$ is replaced by a linear estimate of $\boldsymbol{s}(i)$ obtained from $\boldsymbol{r}(i+1)$ and $\boldsymbol{r}(i)$, as in [18]. More details on the generation of $\{\hat{s}_n(i-1)\}$ and $\{\bar{s}_n^{(j-1)}(i)\}$ will be provided in the sequel.

Assuming that IBI-cancellation and CP-restoration are perfectly executed, $\boldsymbol{y}^{(j)}(i) := [y_0^{(j)}(i), \ldots, y_{N-1}^{(j)}(i)]$ can be considered as a noise-corrupted output of a circular convolution between the channel $\boldsymbol{h}(i)$ and the transmitted symbols $\boldsymbol{s}(i)$, i.e., $\boldsymbol{y}(i) = \mathcal{C}\big(\boldsymbol{h}(i)\big)\boldsymbol{s}(i) + \boldsymbol{\nu}(i)$. For notational simplicity, we suppress the iteration index j for the remainder of this section. Taking the discrete Fourier transform (DFT) of both sides of the previous equation, we obtain the frequency-domain description $\boldsymbol{x}(i) = \boldsymbol{G}(i)\boldsymbol{t}(i) + \boldsymbol{w}(i)$, where $\boldsymbol{x}(i)$, $\boldsymbol{t}(i)$ and $\boldsymbol{w}(i)$ denote the DFTs of $\boldsymbol{y}(i)$, $\boldsymbol{s}(i)$ and $\boldsymbol{\nu}(i)$, respectively, and where $\boldsymbol{G}(i) = \mathcal{D}\big(\boldsymbol{g}(i)\big)$, $\boldsymbol{g}(i)$=$\sqrt{N}\boldsymbol{F}\boldsymbol{h}(i)$, and $\boldsymbol{w}(i) \sim \mathcal{CN}(\boldsymbol{0}, \sigma_w^2\boldsymbol{I})$. We refer to elements in $\boldsymbol{t}(i)$ as *synthetic subcarriers*.

Stacking the mean and variance of each element in $\boldsymbol{s}(i)$ into the vectors $\overline{\boldsymbol{s}}(i)$ and $\boldsymbol{v}_s(i)$, respectively, we can define $\overline{\boldsymbol{t}}(i) := \mathrm{E}[\boldsymbol{t}(i)] = \boldsymbol{F}\overline{\boldsymbol{s}}(i)$ and $\boldsymbol{R}_{\boldsymbol{tt}}(i) := \mathrm{cov}(\boldsymbol{t}(i)) = \boldsymbol{F}\,\mathcal{D}\big(\boldsymbol{v}_{\boldsymbol{s}}(i)\big)\boldsymbol{F}^H$. To simplify the equalization task, we use the approximation $\tilde{\boldsymbol{R}}_{\boldsymbol{tt}}(i) := \mathcal{D}\big(\mathrm{diag}\left(\boldsymbol{R}_{\boldsymbol{tt}}(i)\right)\big)$ in place of the true correlation matrix $\boldsymbol{R}_{\boldsymbol{tt}}(i)$. This approximation is perfect (i.e., $\tilde{\boldsymbol{R}}_{\boldsymbol{tt}}(i) = \boldsymbol{R}_{\boldsymbol{tt}}(i)$) when the elements of $\boldsymbol{s}(i)$ are i.i.d. Note that the APPLE algorithm proposed in [5], [6] makes the more severe approximation $\tilde{\boldsymbol{R}}_{\boldsymbol{tt}}(i) = \boldsymbol{I}$.

Taking $\overline{\boldsymbol{t}}(i)$ and $\tilde{\boldsymbol{R}}_{\boldsymbol{tt}}(i)$ as priors, the minimum mean square error (MMSE) estimate of $\boldsymbol{t}(i)$ is [16]

$$\hat{\boldsymbol{t}}(i) = \overline{\boldsymbol{t}}(i) + \tilde{\boldsymbol{R}}_{\boldsymbol{tt}}(i)\boldsymbol{G}^H(i)\boldsymbol{R}_{\boldsymbol{xx}}^{-1}\left(\boldsymbol{x}(i) - \boldsymbol{G}(i)\overline{\boldsymbol{t}}(i)\right) \tag{3}$$

for $\boldsymbol{R_{xx}} = \boldsymbol{G}(i)\tilde{\boldsymbol{R}}_{\boldsymbol{tt}}(i)\boldsymbol{G}^H(i) + \sigma_w^2\boldsymbol{I}$. A straightforward examination of $\boldsymbol{R_{tt}}(i)$ reveals that the elements on its diagonal equal $v_t(i) = \frac{1}{N}\sum_{n=0}^{N-1} v_{s_n}(i)$, so that $\tilde{\boldsymbol{R}}_{\boldsymbol{tt}}(i) = v_t(i)\boldsymbol{I}$. Therefore, from (3), the kth element in $\hat{\boldsymbol{t}}(i)$ can be conveniently computed via

$$\hat{t}_k(i) = \overline{t}_k(i) + \underbrace{\frac{v_t(i)g_k^*(i)}{v_t(i)|g_k(i)|^2 + \sigma_w^2}}_{:=\, b_k(i)} \left(x_k(i) - g_k(i)\overline{t}_k(i)\right). \quad (4)$$

The time-domain symbol estimates are then obtained via inverse FFT as $\hat{\boldsymbol{s}}(i) = \boldsymbol{F}^{-1}\hat{\boldsymbol{t}}(i)$. Approximating the symbol estimation error distribution as Gaussian (invoking central limit theorem [20] arguments for large enough N), we can generate priors for the MAP decoder via

$$p(\hat{s}_n(i)|s_n(i)=s) = \frac{1}{\sqrt{\pi\sigma^2_{n,i|s}}}\exp\left(\frac{-(\hat{s}_n(i)-u_{n,i|s})^2}{\sigma^2_{n,i|s}}\right), \quad (5)$$

where $u_{n,i|s} := \mathrm{E}\{\hat{s}_n(i)|s_n(i)=s\}$ and $\sigma^2_{n,i|s} := \mathrm{var}\{\hat{s}_n(i)|s_n(i)=s\}$ for $s \in \mathcal{S}$. It can be shown [21, App. 2.A] that $u_{n,i|s}$ and $\sigma^2_{n,i|s}$ can be written as $u_{n,i|s} = \overline{s}_n(i) + \frac{s-\overline{s}_n(i)}{N}\sum_{k=0}^{N-1} b_k(i)g_k(i)$, and $\sigma^2_{n,i|s} \approx \frac{1}{N}\sum_{k=0}^{N-1}|b_k(i)|^2\Big(|g_k(i)|^2\tilde{v}_n(i) + \sigma_w^2\Big)$, where $\tilde{v}_n(i) := \frac{1}{N}\sum_{k\neq n} v_{s_k}(i)$ and where $b_k(i)$ was defined in (4). The latter approximation follows from the use of $\tilde{\boldsymbol{R}}_{\boldsymbol{tt}}(i)$ in place of $\boldsymbol{R_{tt}}(i)$, as in (3).

Finally, we consider the update of *a priori* information for the MMSE estimator using the extrinsic information provided by the decoder. As in [4], the soft feedback information can be expressed as $\{P(s_n(i)=s|\hat{\boldsymbol{s}}(i))\}_{s\in\mathcal{S}}$, which can be used to update the mean and variance of $s_n(i)$ as follows:

$$\bar{s}_n(i) := \mathrm{E}\{s_n(i)|\hat{\boldsymbol{s}}(i)\} = \sum_{s\in\mathcal{S}} sP(s_n(i)=s|\hat{\boldsymbol{s}}(i)) \quad (6)$$

$$v_{s_n(i)} := \mathrm{var}\{s_n(i)|\hat{\boldsymbol{s}}(i)\} = \sum_{s\in\mathcal{S}} |s-\bar{s}_n(i)|^2 P(s_n(i)=s|\hat{\boldsymbol{s}}(i)). \quad (7)$$

V. Adaptive Frequency-Domain Channel Estimation

In this section, we propose an adaptive frequency-domain channel estimation (AFDCE) technique that works in conjunction with our IFDE. Unlike previous approaches to single-carrier FDCE systems, which are either exclusively pilot-aided [13], [14] or partially pilot-aided [15], ours is exclusively decision-directed. The proposed FDCE consists of two stages. First, per-tone Kalman filtering is used to track the channel in the frequency-domain, and second, across-tone filtering is used to refine the channel estimates. This two-stage approach is motivated by a significant reduction in complexity relative to joint Kalman filtering of all tones. In addition, we propose a method to track the AR model coefficients, since in practice they will be unknown and time-varying.

A. Per-Tone Channel Estimation

In this section, we assume a wide sense stationary uncorrelated scattering (WSSUS) channel, in which case we can write $\mathrm{E}[h_l(i)h_{l+p}(i+q)] = \sigma^2_{h_l}\rho_q\delta_p$, where $\{\rho_q\}$ is the time-domain autocorrelation sequence (normalized so that $\rho_0 = 1$) and where $\{\sigma^2_{h_l}\}_{l=0}^{N_h-1}$ is the ISI-power profile. A state-space model for the kth frequency bin can be formulated using an M-th order AR model as (see [21, App. 2.C]):

$$\underline{\boldsymbol{g}}_k(i) = \boldsymbol{A}\underline{\boldsymbol{g}}_k(i-1) + \underline{\boldsymbol{\eta}}_k(i), \quad (8)$$

$$x_k(i) = g_k(i)t_k(i) + w_k(i) \quad (9)$$

where we have approximated the synthetic subcarriers corresponding to the hard symbol decisions by the error-free quantities $\{t_k(i)\}_{k=0}^{N-1}$. Here we used $\underline{\boldsymbol{g}}_k(i) = [g_k(i),\ldots,g_k(i-M+1)]^T$, $\underline{\boldsymbol{\eta}}_k(i) = [\eta_k(i),0,\ldots,0]^T$, $\eta_k(i) \sim \mathcal{CN}(0,\sigma_\eta^2)$, and $\boldsymbol{A} = \begin{bmatrix}\boldsymbol{\alpha}^T & \alpha_M \\ \boldsymbol{I} & \boldsymbol{0}\end{bmatrix}$, where $\boldsymbol{\alpha} := [\alpha_1,\alpha_2,\ldots,\alpha_{M-1}]^T$ and $\{\alpha_m\}_{m=1}^M$ denote the AR model coefficients. Given the channel statistics, $\{\alpha_l\}_{l=1}^M$ and σ_η^2 can be obtained via the Yule-Walker method [16].

Kalman filtering [16] can then be carried out iteratively through (10)-(14). For this we define $\mathcal{X}_{k,i} := \{\boldsymbol{x}_k(j)\}_{j=0}^i$ as the set of observations up to the i^{th} block and $\boldsymbol{P}_k(i) := \mathrm{E}\left[\boldsymbol{\varepsilon}_k(i)\boldsymbol{\varepsilon}_k^H(i)\right]$ where $\boldsymbol{\varepsilon}_k(i) := \underline{\boldsymbol{g}}_k(i) - \underline{\hat{\boldsymbol{g}}}_k(i|\mathcal{X}_{k,i-1})$. Also, we define $\boldsymbol{\sigma}_\eta^2 := [\sigma_\eta^2,0,\ldots,0]^T$ and use $\boldsymbol{i}_k$ to denote the kth column of the identity matrix. Then, assuming that $\boldsymbol{P}_k(i)$ and $\underline{\hat{\boldsymbol{g}}}_k(i|\mathcal{X}_{k,i-1})$ are available from the previous block, and initializing (i.e., $i=0$) with $\underline{\hat{\boldsymbol{g}}}_k(0|\mathcal{X}_{k,0}) = \boldsymbol{0}$ and $\boldsymbol{P}_k(0) = \boldsymbol{R} := \mathrm{E}\{\underline{\boldsymbol{g}}_k(0)\underline{\boldsymbol{g}}_k^H(0)\}$,

$$\boldsymbol{q}_k(i) = \boldsymbol{P}_k(i)t_k(i)^*\boldsymbol{i}_1\left(t_k(i)\boldsymbol{i}_1^H\boldsymbol{P}_k(i)\boldsymbol{i}_1 t_k^*(i) + \sigma_w^2\right)^{-1} \quad (10)$$

$$e_k(i) = x_k(i) - t_k(i)\boldsymbol{i}_1^H\underline{\hat{\boldsymbol{g}}}_k(i|\mathcal{X}_{k,i-1}) \quad (11)$$

$$\underline{\hat{\boldsymbol{g}}}_k(i|\mathcal{X}_{k,i}) = \underline{\hat{\boldsymbol{g}}}_k(i|\mathcal{X}_{k,i-1}) + e_k(i)\boldsymbol{q}_k(i) \quad (12)$$

$$\underline{\hat{\boldsymbol{g}}}_k(i+1|\mathcal{X}_{k,i}) = \boldsymbol{A}\underline{\hat{\boldsymbol{g}}}_k(i|\mathcal{X}_{k,i}) \quad (13)$$

$$\boldsymbol{P}_k(i+1) = \boldsymbol{A}(\boldsymbol{I} - \boldsymbol{q}_k(i)t_k(i)\boldsymbol{i}_1^H)\boldsymbol{P}_k(i)\boldsymbol{A}^T + \mathcal{D}(\boldsymbol{\sigma}_\eta^2). \quad (14)$$

B. Across-Tone Channel Refinement

Because the channel tracking scheme in Section V-A is done on a per-tone basis, it has significantly less complexity than the full Kalman filtering (i.e., across all tones). However, it is suboptimal because it ignores correlation between the elements of $\boldsymbol{g}(i)$. In this section, we propose a computationally efficient means of refining the per-tone channel estimates that leverages the correlation structure of $\boldsymbol{g}(i)$.

Say that $\hat{\boldsymbol{g}}(i|\mathcal{X}_i) := [\hat{g}_0(i|\mathcal{X}_{0,i}),\ldots,\hat{g}_{N-1}(i|\mathcal{X}_{N-1,i})]^T$ denotes the per-tone estimates of $\boldsymbol{g}(i)$ generated via (10)-(14), and that $\boldsymbol{\varepsilon}(i) := \boldsymbol{g}(i) - \hat{\boldsymbol{g}}(i|\mathcal{X}_i)$ denotes the per-tone estimation error. The linear refinement $\breve{\boldsymbol{g}}(i) = \boldsymbol{B}\hat{\boldsymbol{g}}(i|\mathcal{X}_i)$ that minimizes the MSE $\mathrm{E}\{\|\boldsymbol{g}(i) - \breve{\boldsymbol{g}}(i)\|^2\}$ can be derived as follows. Assuming that $\boldsymbol{\varepsilon}(i)$ is zero-mean with $\mathrm{E}\{\boldsymbol{\varepsilon}(i)\boldsymbol{\varepsilon}^H(i)\} = \sigma_\varepsilon^2\boldsymbol{I}$ and that $\mathrm{E}\{\boldsymbol{\varepsilon}(i)\boldsymbol{g}^H(i)\} = \boldsymbol{0}$, the orthogonality principle of MMSE estimation (i.e., $\mathrm{E}\{(\boldsymbol{g}(i) - \breve{\boldsymbol{g}}(i))\hat{\boldsymbol{g}}^H(i|\mathcal{X}_i))\} = \boldsymbol{0}$) straightforwardly implies that $\boldsymbol{B} = \boldsymbol{R_{gg}}\left(\boldsymbol{R_{gg}} + \sigma_\varepsilon^2\boldsymbol{I}\right)^{-1}$ with $\boldsymbol{R_{gg}} := \mathrm{E}\{\boldsymbol{g}(i)\boldsymbol{g}^H(i)\}$. For our WSSUS channel, we show in [21, App. 2.C] that $\mathrm{E}[g_k(i)g_p(i)^*] = \sum_{l=0}^{N_h-1}\sigma^2_{h_l}e^{-j\frac{2\pi}{N}(k-p)l}$, which implies that $\boldsymbol{R_{gg}} = \boldsymbol{F}\,\mathcal{D}(N\boldsymbol{\sigma}_h^2)\boldsymbol{F}^H$ for $\boldsymbol{\sigma}_h^2 := [\sigma^2_{h_0},\ldots,\sigma^2_{h_{N_h-1}},0,\ldots,0]^T \in \mathbb{R}^N$. Writing $\boldsymbol{B} = \boldsymbol{F}\,\mathcal{D}(\boldsymbol{\gamma})\boldsymbol{F}^H$ for $\boldsymbol{\gamma} := [\gamma_0,\gamma_1,\ldots,\gamma_{N-1}]^T$ and $\gamma_l = \left(1 + \sigma_\varepsilon^2/(N\sigma^2_{h_l})\right)^{-1}$ shows that MMSE refinement can be accomplished using a fast FFT-based algorithm. In the case that $\{\sigma_\varepsilon^2/\sigma^2_{h_l}\}_{l=0}^{N_h}$ are

TABLE I
COMPUTATIONAL COMPLEXITY

Task	Real Multiplications	Real Additions
IFDE	$8N\log_2(N)+19N$	$8N\log_2(N)+13N$
APPLE	$8N\log_2(N)+11N$	$8N\log_2(N)+10N$
MF	$14N\log_2(N)+12N+24N_h\log_2(2N_h)$	$14N\log_2(N)+8N+24N_h\log_2(2N_h)$
AFDCE	$N(6M^2+14M+9)$	$N(5M^2+9M+6)$
(from ATCR)	$+8MN\log_2(N)$	$+8MN\log_2(N)$
(from ATARMC)	$+M^2N+3MN+\frac{2}{3}M^3+3M^2+2N$	$+M^2N+3MN+\frac{2}{3}M^3+2M^2+2N$
LMS-FDCE	$8N\log_2(N)+6N$	$8N\log_2(N)+6N$

unknown, the high-SNR approximation $\sigma_\varepsilon^2 \to 0$ can be used, which implies that $\gamma_l = 1$ for $l \in \{0,\ldots,N_h-1\}$ and $\gamma_l = 0$ otherwise. In any case, it can be shown that the refined-estimate error $\boldsymbol{\epsilon}(i) := \boldsymbol{g}(i) - \breve{\boldsymbol{g}}(i)$ has covariance $\boldsymbol{R}_{\boldsymbol{\epsilon}\boldsymbol{\epsilon}} = \left(\boldsymbol{R}_{\boldsymbol{g}\boldsymbol{g}}^{-1} + \sigma_\varepsilon^{-2}\boldsymbol{I}\right)^{-1} = \boldsymbol{F}\,\mathcal{D}(\boldsymbol{\zeta})\boldsymbol{F}^H$ for $\boldsymbol{\zeta} = [\zeta_0,\zeta_1,\ldots,\zeta_{N-1}]^T$ and $\zeta_l = \left(1/(N\sigma_{h_l}^2) + 1/\sigma_\varepsilon^2\right)^{-1}$.

For practical IFDE, the refined channel estimates $\{\breve{g}_k(i)\}_{k=0}^{N-1}$ are used in place of $\{g_k(i)\}_{k=0}^{N-1}$ in (4). In this case, $\boldsymbol{x}(i) = \mathcal{D}(\breve{\boldsymbol{g}}(i))\boldsymbol{t}(i) + \boldsymbol{z}(i)$, where the effective noise $\boldsymbol{z}(i) := \mathcal{D}(\boldsymbol{\epsilon}(i))\boldsymbol{t}(i) + \boldsymbol{w}(i)$ includes channel estimation error. Assuming $\boldsymbol{\epsilon}(i)$, $\boldsymbol{t}(i)$, and $\boldsymbol{w}(i)$ are uncorrelated and treating $\boldsymbol{t}(i)$ as unknown (i.e., $\boldsymbol{R}_{\boldsymbol{t}\boldsymbol{t}}(i) = \boldsymbol{I}$) yields $\boldsymbol{R}_{\boldsymbol{z}\boldsymbol{z}} = \sigma_z^2\boldsymbol{I}$ with $\sigma_z^2 = \sum_{l=0}^{N-1}\zeta_l + \sigma_w^2$, which is then used for σ_w^2 in (4).

So far we have discussed across-tone refinement of a single vector $\hat{\boldsymbol{g}}(i|\mathcal{X}_i)$. Merging the across-tone refinement procedure with the per-tone Kalman algorithm (10)-(14) requires that, for each i, across-tone refinement is applied to the entire M-sample block $\hat{\underline{\boldsymbol{G}}}(i|\mathcal{X}_i) := [\hat{\underline{\boldsymbol{g}}}_0(i|\mathcal{X}_{0,i}),\ldots,\hat{\underline{\boldsymbol{g}}}_{N-1}(i|\mathcal{X}_{N-1,i})]^T$ and that the refined outputs are used in the forward-prediction step (13). In total, this procedure consumes $2M$ FFTs at each index i.

C. Adaptive Tracking of AR Model Coefficients

When the Doppler spread of the channel is unknown or time-varying, AR model coefficient estimates can be obtained by tracking the channel statistics. Note that (8) and the definition of $\boldsymbol{A}$ imply $g_k(i) = \boldsymbol{\alpha}^T\underline{\boldsymbol{g}}_k(i-1) + \eta_k(i)$ for $\boldsymbol{\alpha} := [\alpha_1,\alpha_2,\ldots,\alpha_M]^T$. For a stationary channel with $\boldsymbol{\Sigma} := \mathrm{E}\{\underline{\boldsymbol{g}}_k(i)\underline{\boldsymbol{g}}_k^H(i)\}$ and $\boldsymbol{\varrho} := \mathrm{E}\{g_k^*(i+1)\underline{\boldsymbol{g}}_k(i)\}$, the Yule-Walker equations [16] specify that $\boldsymbol{\alpha} = \boldsymbol{\Sigma}^{-1}\boldsymbol{\varrho}$. When the statistics are slowly varying, the latter equation can be used to track the unknown AR coefficients $\boldsymbol{\alpha}(i)$ via estimates of $\boldsymbol{\Sigma}(i)$ and $\boldsymbol{\varrho}(i)$. In particular, we can use the recursive estimates $\hat{\boldsymbol{\varrho}}(i) = \lambda\hat{\boldsymbol{\varrho}}(i-1) + \frac{(1-\lambda)}{N}\sum_{k=0}^{N-1}\hat{g}_k^*(i)\hat{\underline{\boldsymbol{g}}}_k(i-1)$ and $\hat{\boldsymbol{\Sigma}}(i) = \lambda\hat{\boldsymbol{\Sigma}}(i-1) + \frac{(1-\lambda)}{N}\sum_{k=0}^{N-1}\hat{\underline{\boldsymbol{g}}}_k(i-1)\hat{\underline{\boldsymbol{g}}}_k^H(i-1)$, where $\lambda \in (0,1)$ is a suitably chosen forgetting factor, to generate the AR-coefficient estimate $\hat{\boldsymbol{\alpha}}(i) = \hat{\boldsymbol{\Sigma}}^{-1}(i)\hat{\boldsymbol{\varrho}}(i)$. Given estimates of $g_k(i)$, $\boldsymbol{\alpha}$ and $\underline{\boldsymbol{g}}_k(i-1)$, the AR model suggests that an estimate of $\sigma_\eta^2(i)$ can be obtained via $\hat{\sigma}_\eta^2(i) = \lambda\hat{\sigma}_\eta^2(i-1) + \frac{(1-\lambda)}{N}\sum_{k=0}^{N-1}|\hat{\eta}_k(i)|^2$ for $\hat{\eta}_k(i) = \hat{g}_k(i) - \hat{\boldsymbol{\alpha}}^T(i)\hat{\underline{\boldsymbol{g}}}_k(i-1)$. A related method of tracking basis expansion coefficients was proposed in [9] for $M=1$ and without the averaging over k.

VI. IMPLEMENTATIONAL CONSIDERATIONS

A. Block Overlapping

Due to causal channel dispersion and lack of CP, the N_h-1 symbols at the end of the block contribute relatively little energy to the observation and hence are more difficult to estimate. MAP-decoding error propagation also makes their neighboring symbols somewhat difficult to estimate. For these reasons, we choose to keep only the leftmost $N_d = N-2N_h$ symbol estimates in each block. Recalling that N_d is the block shift interval, it can be seen that every symbol will appear in the beginning of exactly one block. A similar idea was proposed for CDMA multiuser detection in [22].

B. Complexity Analysis

The computational complexities of IFDE, AFDCE, and related algorithms from the literature are reported in Table I. For the symbol detection algorithms,[3] Table I reports the number of real mults/adds required per-iteration to yield N time-domain symbol estimates. Since the APPLE/MF algorithm from [5], [6] alternates between the APPLE and MF tasks depending on the system state, an exact complexity count is impossible. But if we assume that APPLE/MF complexity falls midway between that of APPLE and MF, then it can be seen that IFDE is slightly cheaper.

For the CE algorithms, Table I reports the number of real mults/adds required to yield N frequency-domain channel coefficient estimates. In the typical case of large block-length N and small AR-model order M (e.g., $M=2$), the dominant complexity terms[4] in Table I indicate that the complexity of AFDCE is about M times that of the LMS-based FDCE algorithm from [23]. In reporting AFDCE complexity, we isolated the costs of across-tone channel refinement (ATCR) and adaptive tracking of AR model coefficients (ATARMC).

VII. NUMERICAL RESULTS

A. Setup

We considered a single-carrier non-CP system, where the information bit sequence was encoded with the code gen-

[3]Complexity is specified *per-iteration* since both APPLE/MF and IFDE require approximately the same number of iterations before saturating. Also, Table I includes the cost of generating priors for MAP-decoding, but not the cost of computing priors for MMSE-equalization, since this latter cost is identical for APPLE/MF and IFDE.

[4]We assumed radix-2 FFTs that cost $2N\log_2(N)$ real multiplications and real additions per real N-vector and $4N\log_2(N)$ real multiplications and real additions per complex N-vector.

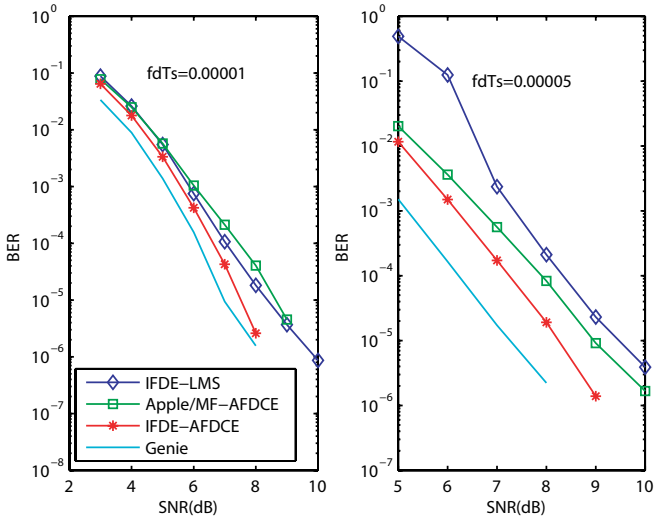

Fig. 2. BER versus SNR for WSSUS Rayleigh channels.

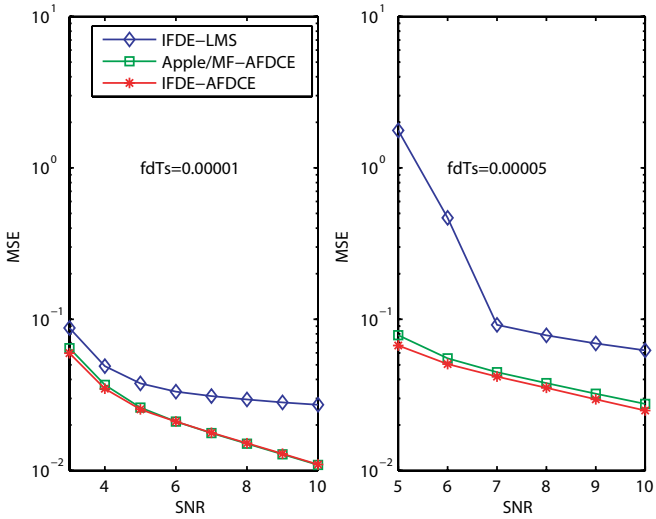

Fig. 3. Channel-estimate-MSE versus SNR for WSSUS Rayleigh channels.

erator $G(D) = (1 + D^2, 1 + D + D^2)$ and Gray-mapped to QPSK. Channel realizations were generated using Jakes' model with delay spread N_h, exponential power profile $\sigma^2_{N_l} = e^{-l/N_l} / \sum_{l'=0}^{N_h-1} e^{-l'/N_l}$, and autocorrelation $\rho_q = \mathcal{J}_0(2\pi f_d T_s N q)$, where $\mathcal{J}_0(\cdot)$ denotes the 0th-order Bessel function of the first kind. The factor "N" appears in ρ_q because "q" denotes time-lag in blocks. We focused on (single-sided) normalized Doppler spread $f_d T_s \in \{0.00001, 0.00005\}$ and delay spread $N_h = 128$, which, e.g., corresponds to Doppler spread $f_d \in \{100, 500\}$Hz and delay spread of $12.8\ \mu$s at sampling rate $T_s^{-1} = 10$ MHz. We used block-length $N = 512$, block-shift interval $N_d = 256$, AR model order $M = 2$, and $N_{iter} = 5$ iterations for both APPLE/MF and IFDE (since more iterations did not significantly improve performance). For AFDCE across-tone channel-refinement, the "high-SNR" approximation from Section V-B was used, avoiding the need to know σ^2_ε. Our results represent the average of 1000 independent experiments of 51200 consecutive data symbols. Each length-51200 data-symbol sequence was preceded by a length-N (random QPSK) pilot-symbol sequence for CE initialization.

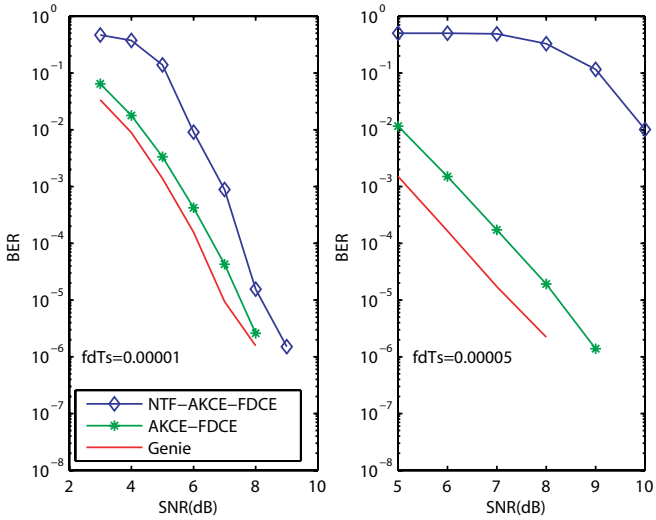

Fig. 4. BER versus SNR for WSSUS Rayleigh channels.

B. Results

First, we compared our proposed IFDE/AFDCE to IFDE with a perfectly known channel. Figure 2 shows that our IFDE/AFDCE performed within 1dB of this genie-aided bound. Next, we compared our IFDE and AFDCE algorithms to the most closely related frequency-domain equalization and channel estimation algorithms in the literature. In one test, we combined our IFDE with the LMS-based FDCE algorithm from [23]. For this LMS-based FDCE algorithm, we empirically chose step-size $\mu = 0.1$ when $f_d T_s = 0.00001$, and $\mu = 0.5$ when $f_d T_s = 0.00005$, since no optimal choice of μ was specified in [23]. The resulting steady-state BER and channel-estimation-MSE are reported in Fig. 2 and Fig. 3, respectively, where it can be seen that our proposed IFDE/AFDCE outperformed the IFDE/LMS combination throughout the SNR range, and more significantly so at higher Doppler. In another test, we combined our AFDCE with the APPLE-MF equalization algorithm from [5], [6]. Figures 2 and 3 show that our proposed IFDE/AFDCE outperforms APPLE-MF/AFDCE throughout the SNR range.

To investigate the effect of the across-tone channel refinement (ATCR) procedure proposed in Section V-B, we plotted BER versus SNR with and without ATCR in Fig. 4. There it can be seen that the gain of ATCR is significant throughout the SNR range, despite the use of the high-SNR approximation.

In Fig. 5, we again compared the performance of our IFDE/AFDCE combination to IFDE/LMS, but this time we used an adaptive-step-size version of the LMS-based FDCE from [23] and tested the algorithms with a non-stationary channel. For this, we used a channel where $f_d T_s = 0.00001$ for the first 51200 symbols, $f_d T_s = 0.00005$ for the last 51200 symbols, and where the Doppler spectrum smoothly transitions between these cases during the middle 51200 symbols. Figure 5 shows that IFDE/AFDCE achieved lower channel-estimation-MSE than IFDE/LMS and that IFDE/AFDCE has the ability to adapt to varying channel statistics while maintaining excellent BER performance.

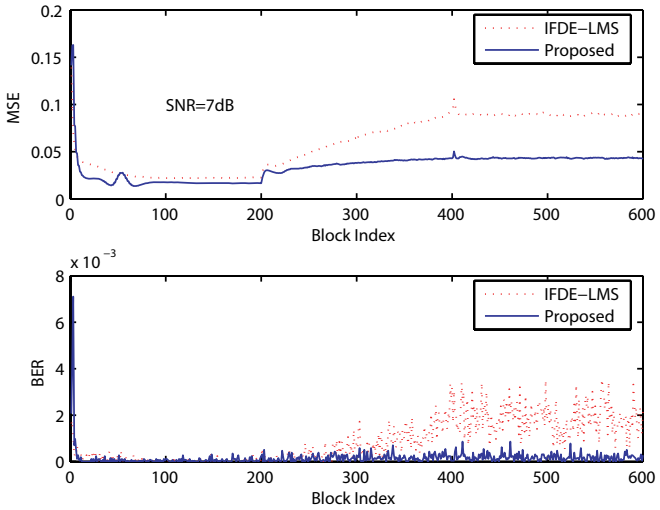

Fig. 5. Channel-estimate-MSE and BER versus block index at SNR= 7dB for a non-stationary Rayleigh channel which transitions from $f_d T_s = 0.00001$ to $f_d T_s = 0.00005$.

VIII. Conclusion

In this paper, we presented an algorithm for joint frequency-domain equalization and channel estimation appropriate for the reception of single-carrier non-CP transmissions over time-varying long-delay-spread channels. In particular, we detailed an improved IFDE algorithm based on frequency-domain turbo equalization, and proposed a novel AFDCE with robustness to fast-fading. Numerical results show that the proposed IFDE-plus-AFDCE scheme demonstrates state-of-the-art performance in both stationary and non-stationary channels while maintaining low complexity via its frequency-domain operation. Deeper analytical insights into the convergence behavior of AFDCE will be the subject of future work.

References

[1] D. Falconer, S. Ariyavisitakul, A. Benyamin-Seeyar, and B. Eidson, "Frequency domain equalization for single-carrier broadband wireless systems," *IEEE Commun. Mag.*, vol. 40, no. 4, pp. 58–66, Apr. 2002.

[2] Y. Li, S. McLaughlin, and D. G. M. Cruickshank, "Bandwidth efficient single carrier systems with frequency domain equalisation," *Electron. Lett.*, vol. 41, no. 15, pp. 857–858, July 2005.

[3] C. Douillard, M. Jezequel, C. Berrou, A. Picart, P. Didier, and A. Glavieux, "Iterative correction of intersymbol interference: turbo equalization," *European Trans. Telecommun.*, vol. 6, no. 5, pp. 507–511, Sept.-Oct. 1995.

[4] R. Koetter, A. Singer, and M. Tüchler, "Turbo equalization," *IEEE Signal Processing Mag.*, vol. 21, no. 1, pp. 67–80, Jan. 2004.

[5] M. Tüchler and J. Hagenauer, "Turbo equalization using frequency domain equalizers," in *Proc. Allerton Conf.*, Oct. 2000.

[6] ——, "Linear time and frequency domain turbo equalization," in *Proc. IEEE VTC*, May 2001.

[7] D. Schafhuber, G. Matz, and F. Hlawatsch, "Kalman tracking of time-varying channels in wireless MIMO-OFDM systems," in *Proc. Asilomar Conf.*, Nov. 2003.

[8] D. Schafhuber and G. Matz, "MMSE and adaptive prediction of time-varying channels for OFDM systems," *IEEE Trans. Wireless Commun.*, vol. 4, no. 2, pp. 593–602, 2005.

[9] R. C. Cannizzaro, P. Banelli, and G. Leus, "Adaptive channel estimation for OFDM systems with Doppler spread," in *Proc. IEEE SPAWC*, 2006.

[10] M. Tüchler, R. Otnes, and A. Schmidbauer, "Performance of soft iterative channel estimation in turbo equalization," in *Proc. IEEE ICC.*, May 2002.

[11] S. Song, A. C. Singer, and K.-M. Sung, "Soft input channel estimation for turbo equalization," *IEEE Trans. Signal Processing*, vol. 52, no. 10, pp. 2885–2894, Oct. 2004.

[12] B. Ng, C. Lam, and D. Falconer, "Turbo frequency domain equalization for single-carrier broadband wireless systems," *IEEE Trans. Wireless Commun.*, vol. 6, no. 2, pp. 759–767, Feb. 2007.

[13] S. Jiun, J. Coon, R. J. Piechocki, A. Dowler, A. Nix, M. Beach, S. Armour, and J. McGeehan, "A channel estimation algorithm for MIMO-SCFDE," *IEEE Commun. Lett.*, vol. 8, no. 9, pp. 555–557, 2004.

[14] W. Liu, L. Yang, and L. Hanzo, "Wideband channel estimation and prediction in single-carrier wireless systems," in *Proc. IEEE VTC*, May 2005.

[15] C.-T. Lam, D. D. Falconer, and F. Danilo-Lemoine, "A low complexity frequency domain iterative decision-directed channel estimation technique for single-carrier systems," in *Proc. IEEE VTC*, Apr. 2007, pp. 1966–1970.

[16] S. Haykin, *Adaptive Filter Theory*, 4th ed. Upper Saddle River, NJ: Prentice-Hall, 2001.

[17] D. Kim and G. Stüber., "Residual ISI cancellation for OFDM with application to HDTV broadcasting," *IEEE J. Select. Areas Commun.*, vol. 16, no. 8, pp. 1590–1599, Oct. 1998.

[18] C.-J. Park and G.-H. Im, "Efficient cyclic prefix reconstruction for coded OFDM systems," *IEEE Commun. Lett.*, vol. 8, no. 5, pp. 274–276, May 2004.

[19] J. Hagenauer, E. Offer, and L. Papke, "Iterative decoding of binary block and convolutional codes," *IEEE Trans. Inform. Theory*, vol. 42, no. 2, pp. 429–445, Mar. 1996.

[20] A. Papoulis, *Probability, Random Variables, and Stochastic Processes*, 3rd ed. New York: McGraw-Hill, 1991.

[21] H. Liu, "Frequency-domain equalization of single-carrier communications over doubly selective channels," Ph.D. dissertation, Ohio State University, Columbus, Ohio, 2007.

[22] M. Vollmer, M. Haardt, and J. Götze, "Comparative study of joint-detection techniques for TD-CDMA based mobile radio systems," *IEEE J. Select. Areas Commun.*, vol. 19, no. 8, pp. 1461–1475, Aug. 2001.

[23] M. Morelli, L. Sanguinetti, and U. Mengali, "Channel estimation for adaptive frequency-domain equalization," *IEEE Trans. Wireless Commun.*, vol. 4, no. 5, pp. 2508–2518, 2005.